SUPPORTING MATERIALS

Supplementary Results

Relation between average and modal controllability across graphs

As noted in the main manuscript, in prior work we have observed that average and modal controllability, averaged over nodes, are positively related to one another across brain networks [27]. These data suggest that brains that are structurally predisposed to be effective in moving network dynamics into easy-to-reach states (via average control) are also the brain that are structurally predisposed to be effective in moving network dynamics into difficult-to-reach states (via modal control). Here, we ask whether this positive relationship between average and modal controllability across networks holds in canonical graph models. In the main manuscript, we show scatter plots of average and modal controllability for graph models with Gaussian edge weight distributions. Here we show the complementary results for graph models with the power-law (Fig. 17), streamline counts (Fig. 18), and FA (Fig. 19) weighting schemes. Our results demonstrate that there is no consistent relationship between average and modal controllability across graph models and edge weight distributions; the relation between these two variables depends on both graph topology and graph geometry.

Relation between average and modal controllability across nodes

As noted in the main manuscript, in prior work we have observed that average and modal controllability are inversely related to one another across regions in brain networks, both in non-invasive human neuroimaging data acquired in youth and adults [26, 27] and in tract-tracing data acquire from macaque monkeys [26]. These data suggest that regions of the brain that are structurally predisposed to be effective in moving the brain into easy-to-reach states (via average control) are different from the regions of the brain that are structural predisposed to be effective in moving the brain into difficult-to-reach states (via modal control). We ask the important more general question of whether this inverse relationship between average and modal controllability across nodes holds in canonical graph models. In the main manuscript, we show scatter plots of average and modal controllability for graph models with Gaussian edge weight distributions. Here we show the complementary results for graph models with the power-law (Fig. 20), streamline counts (Fig. 22), and FA (Fig. 21) weighting schemes. Our results demonstrate that the inverse relationship between average and modal controllability holds across graph models and edge weight distributions.

Effect of graph size on variation in network controllability statistics across graph models

To assess the reliability and reproducibility of our results, we next examined the impact of graph size (n = 128, 256, or 512) on network controllability statistics, and their modulation by graph model for the Gaussian edge weight distribution. In this section, we examine how network controllability statistics vary over graphs within a given ensemble, and whether that variation differs as a function of graph model. Following the procedure outlined in the Methods section, for each controllability type, we took the mean of the n sorted controllability values across the n nodes in each graph instance, giving us 100 controllability values averaged over the n regions. For each controllability type, we used four identical edge weight distributions corresponding to fractional anisotropy (FA) and streamline counts (SC) from real brain data, Gaussian distribution, and power law distribution. We observed that global, average, modal, and boundary controllability values for graphs of 256 and 512 nodes largely maintained the same trends as for graphs with 128 nodes (Fig. 23, 24, 25, and 26).

Effect of graph size on nodal variation in network controllability statistics across graph models

Here we again assess the reliability and reproducibility of our results, by examining the impact of graph size (n = 128, 256, or 512) on network controllability statistics, and their modulation by graph model for the Gaussian edge weight distribution. In this section, we examine the nodal variation in network controllability statistics, and ask questions regarding how nodal variation differs across graph models, and between controllability statistics. Following the procedure outlined in the Methods section, for each controllability type we took the mean of the n sorted nodal controllability values across all 100 graphs in a given model ensemble, giving us n controllability values averaged over the graph instances. For each controllability type, we used four identical edge weight distributions corresponding to fractional anisotropy (FA) and streamline counts (SC) from real brain data, Gaussian distribution, and power law distribution. We observed that global, average, modal, and boundary controllability values for graphs of 256 and 512 nodes largely maintained the same trends as for graphs with 128 nodes (Fig. 27, 28, 29, and 30).

Effect of ρ on boundary controllability estimates

In the main text, we provided estimates of boundary controllability using $\rho = 1 \times 10^{-5}$. However, we observe similar estimates of boundary controllability for $\rho = 1 \times 10^{-3}$ and $\rho = 1 \times 10^{-8}$. Here we provide an

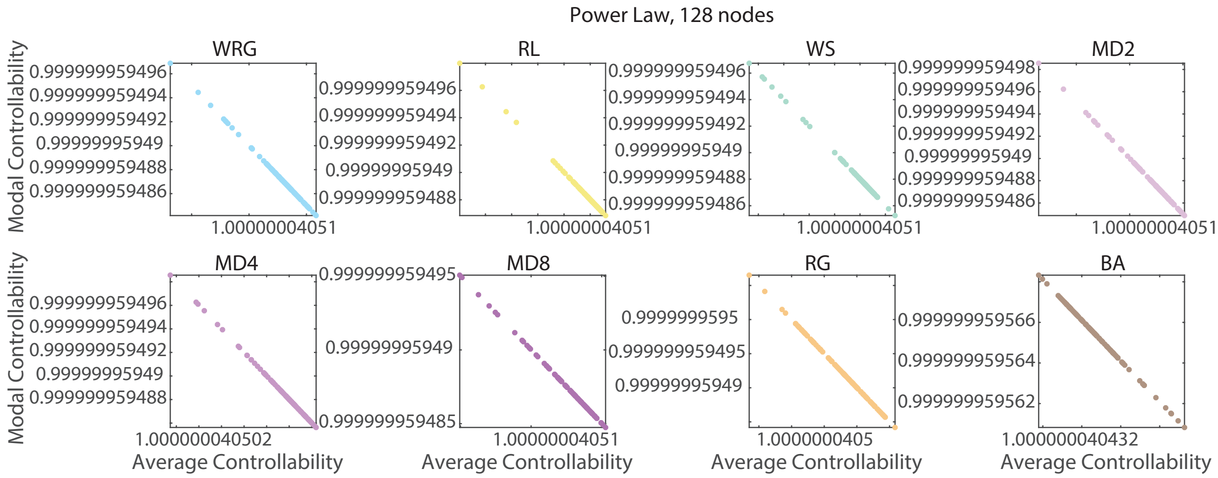

FIG. 17. **Relation between average and modal controllability across graphs for the power-law edge weighting scheme.** Average and modal controllability values were averaged over nodes in each graph model ensemble, and therefore scatterplots show values for each graph in the ensemble. Results are shown for the power-law edge weighting scheme. The eight graph models include the weighted random graph (WRG), the ring lattice (RL), the Watts-Strogatz small-world (WS), the modular graphs (MD2, MD4, MD8), the random geometric (RG), and the Barábasi-Albert preferential attachment (BA) models.

illustrative example for the 128-node graphs using the Fractional Anisotropy edge weight distribution (Fig. 31).

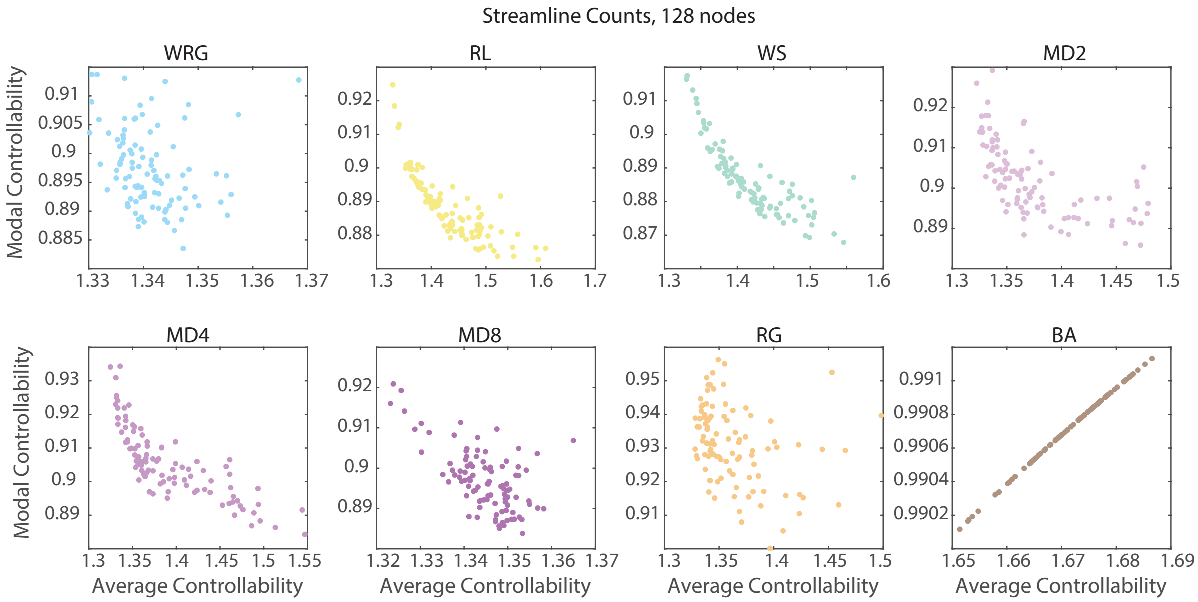

FIG. 18. **Relation between average and modal controllability across graphs for the streamline count edge weighting scheme.** Average and modal controllability values were averaged over nodes in each graph model ensemble, and therefore scatterplots show values for each graph in the ensemble. Results are shown for the streamline count edge weighting scheme. The eight graph models include the weighted random graph (WRG), the ring lattice (RL), the Watts-Strogatz small-world (WS), the modular graphs (MD2, MD4, MD8), the random geometric (RG), and the Barábasi-Albert preferential attachment (BA) models.

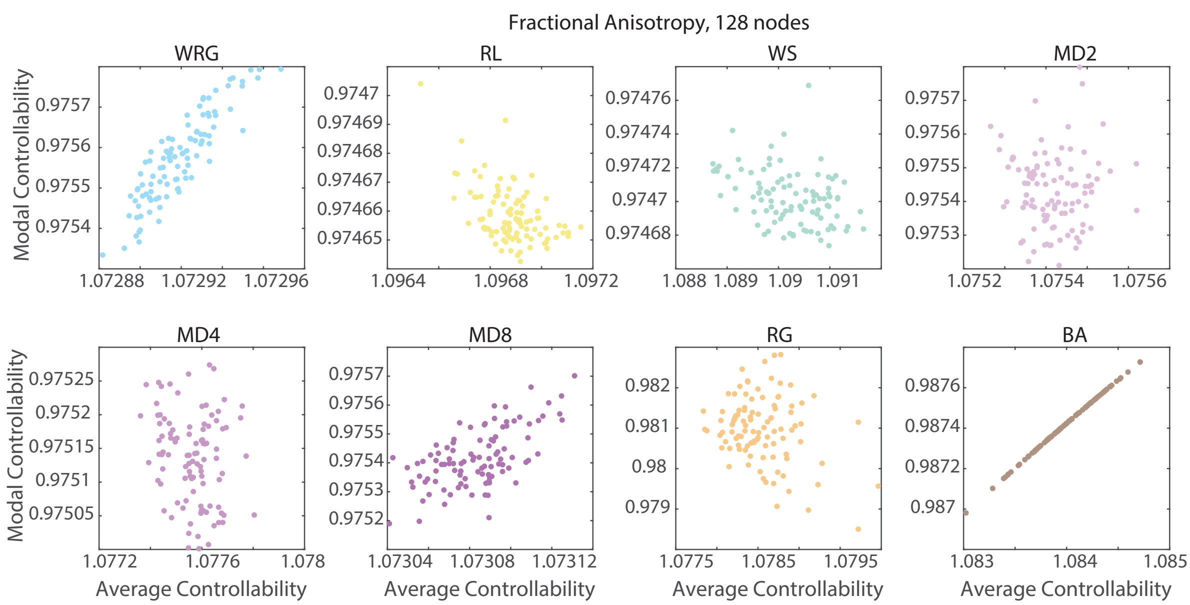

FIG. 19. **Relation between average and modal controllability across graphs for the FA edge weighting scheme.** Average and modal controllability values were averaged over nodes in each graph model ensemble, and therefore scatterplots show values for each graph in the ensemble. Results are shown for the FA edge weighting scheme. The eight graph models include the weighted random graph (WRG), the ring lattice (RL), the Watts-Strogatz small-world (WS), the modular graphs (MD2, MD4, MD8), the random geometric (RG), and the Barábasi-Albert preferential attachment (BA) models.

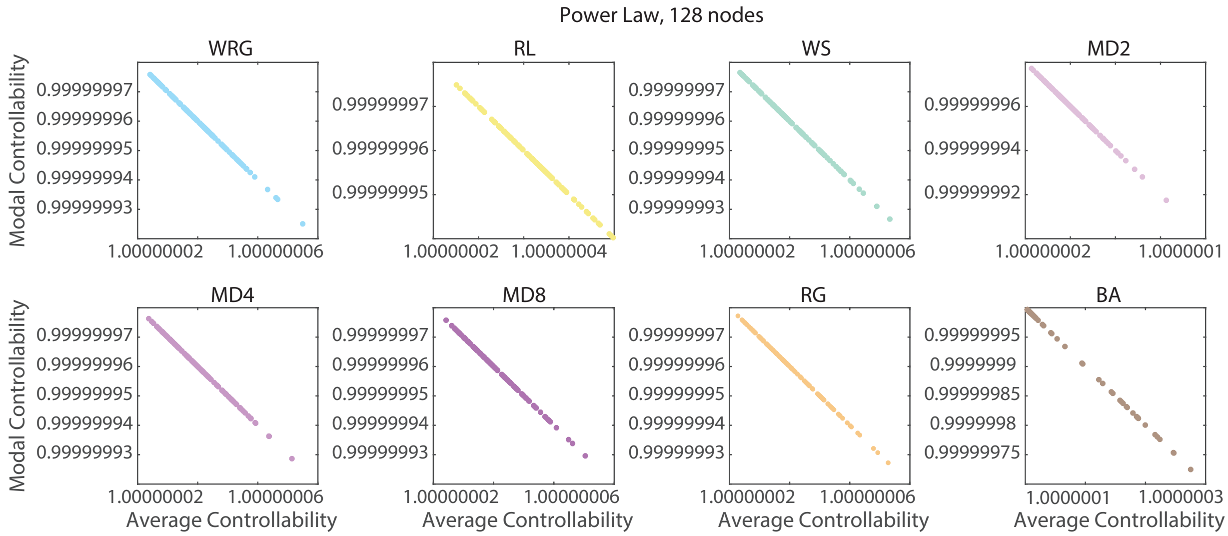

FIG. 20. **Relation between average and modal controllability across nodes for the power-law edge weighting scheme.** Average and modal controllability values were averaged over instances in each graph model ensemble, and therefore scatterplots show values for each node in the graph. Results are shown for the power-law edge weighting scheme. The eight graph models include the weighted random graph (WRG), the ring lattice (RL), the Watts-Strogatz small-world (WS), the modular graphs (MD2, MD4, MD8), the random geometric (RG), and the Barábasi-Albert preferential attachment (BA) models.

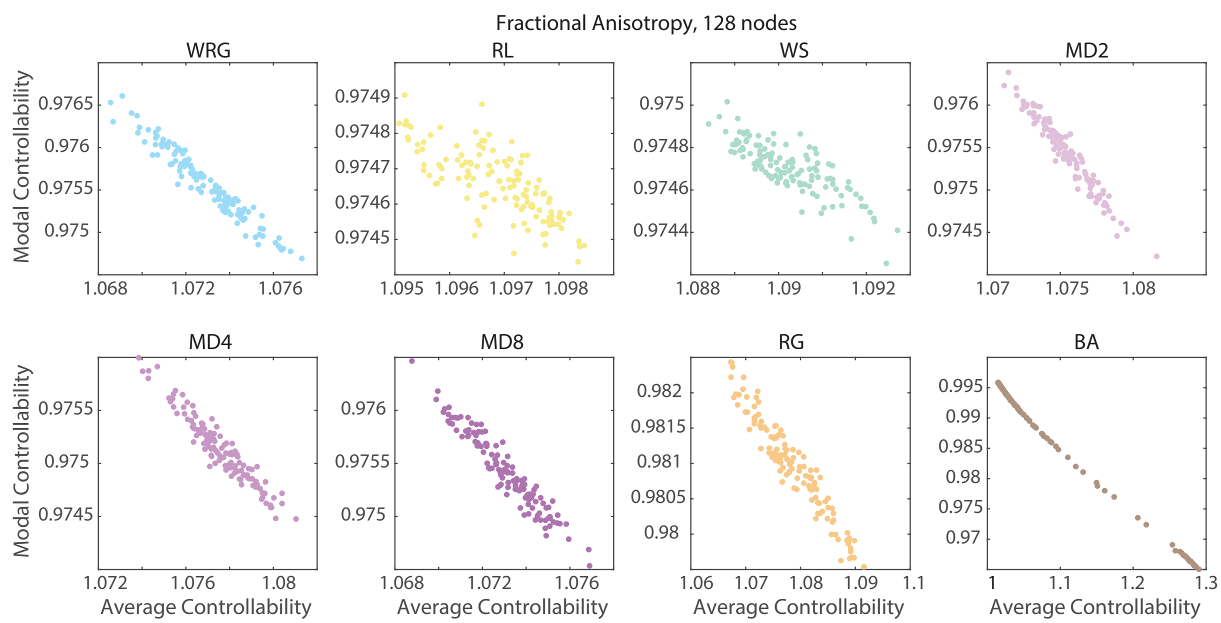

FIG. 21. **Relation between average and modal controllability across nodes for the FA edge weighting scheme.** Average and modal controllability values were averaged over instances in each graph model ensemble, and therefore scatterplots show values for each node in the graph. Results are shown for the FA edge weighting scheme. The eight graph models include the weighted random graph (WRG), the ring lattice (RL), the Watts-Strogatz small-world (WS), the modular graphs (MD2, MD4, MD8), the random geometric (RG), and the Barábasi-Albert preferential attachment (BA) models.

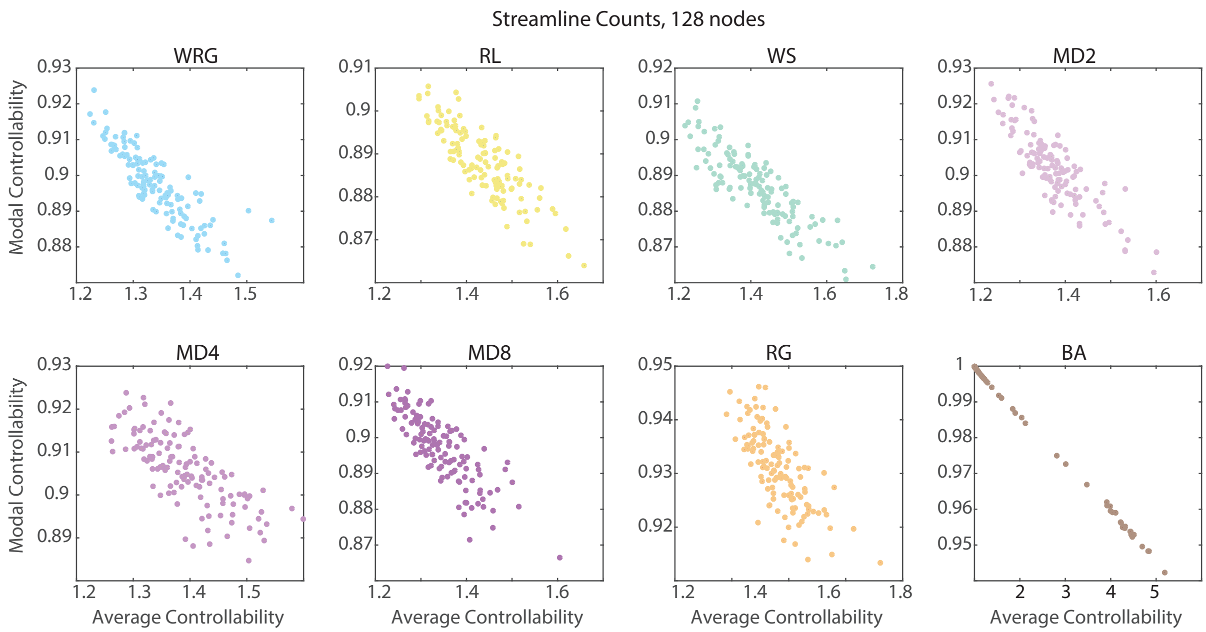

FIG. 22. **Relation between average and modal controllability across nodes for the streamline count edge weighting scheme.** Average and modal controllability values were averaged over instances in each graph model ensemble, and therefore scatterplots show values for each node in the graph. Results are shown for the streamline count edge weighting scheme. The eight graph models include the weighted random graph (WRG), the ring lattice (RL), the Watts-Strogatz small-world (WS), the modular graphs (MD2, MD4, MD8), the random geometric (RG), and the Barábasi-Albert preferential attachment (BA) models.

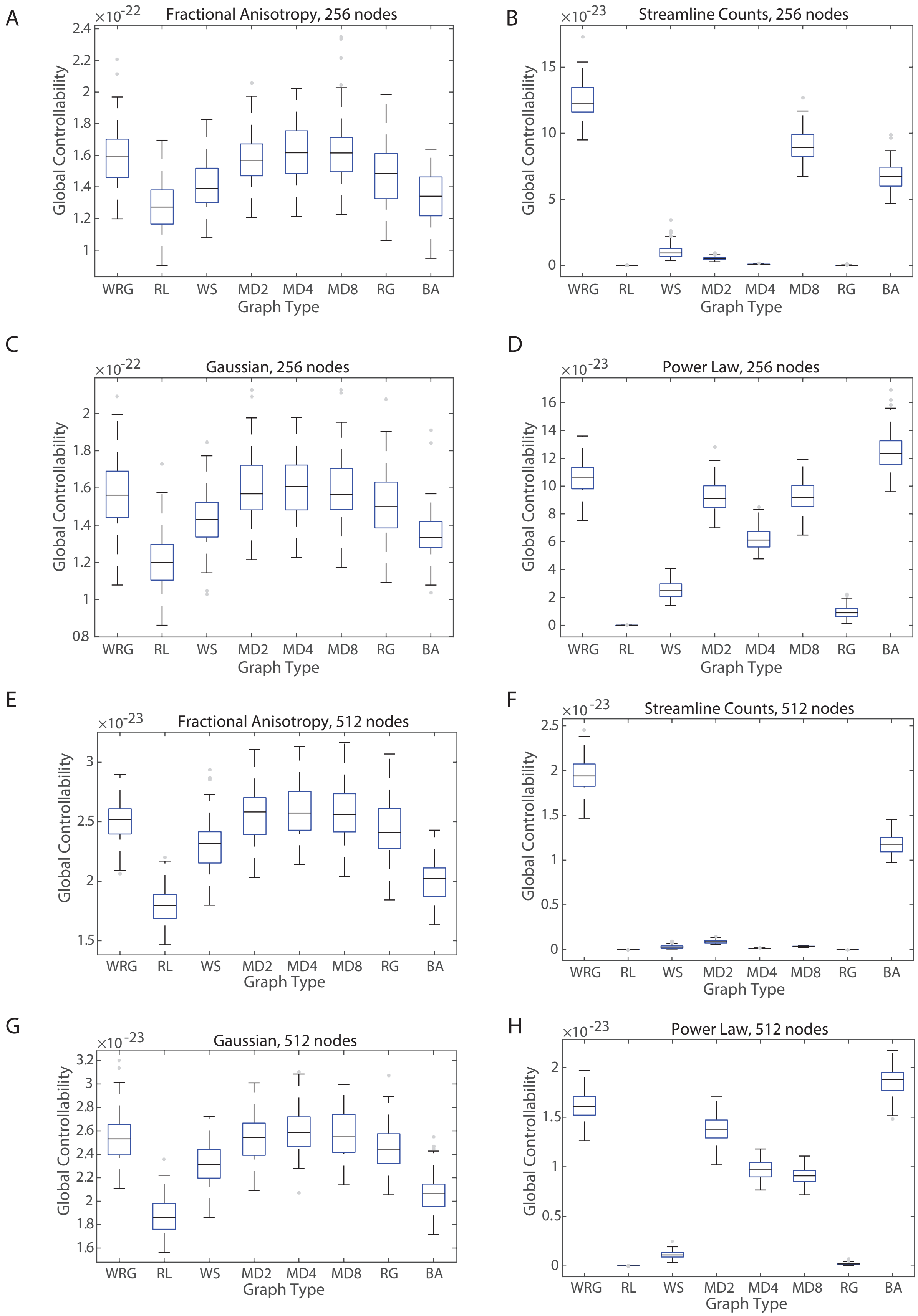

FIG. 23. **Variation in global controllability as a function of edge weighting and graph model.** Global controllability values were averaged over nodes in each graph model ensemble, and therefore boxplots show variation over graphs in the ensemble. Results are shown for four edge weighting schemes: *(A,E)* FA, *(B,F)* streamline counts, *(C,G)* Gaussian, *(D,H)* power-law. The eight graph models include the weighted random graph (WRG), the ring lattice (RL), the Watts-Strogatz small-world (WS), the modular graphs (MD2, MD4, MD8), the random geometric (RG), and the Barábasi-Albert preferential attachment (BA) models. Number of nodes is either 256 *(A-D)* or 512 *(E-H)*.

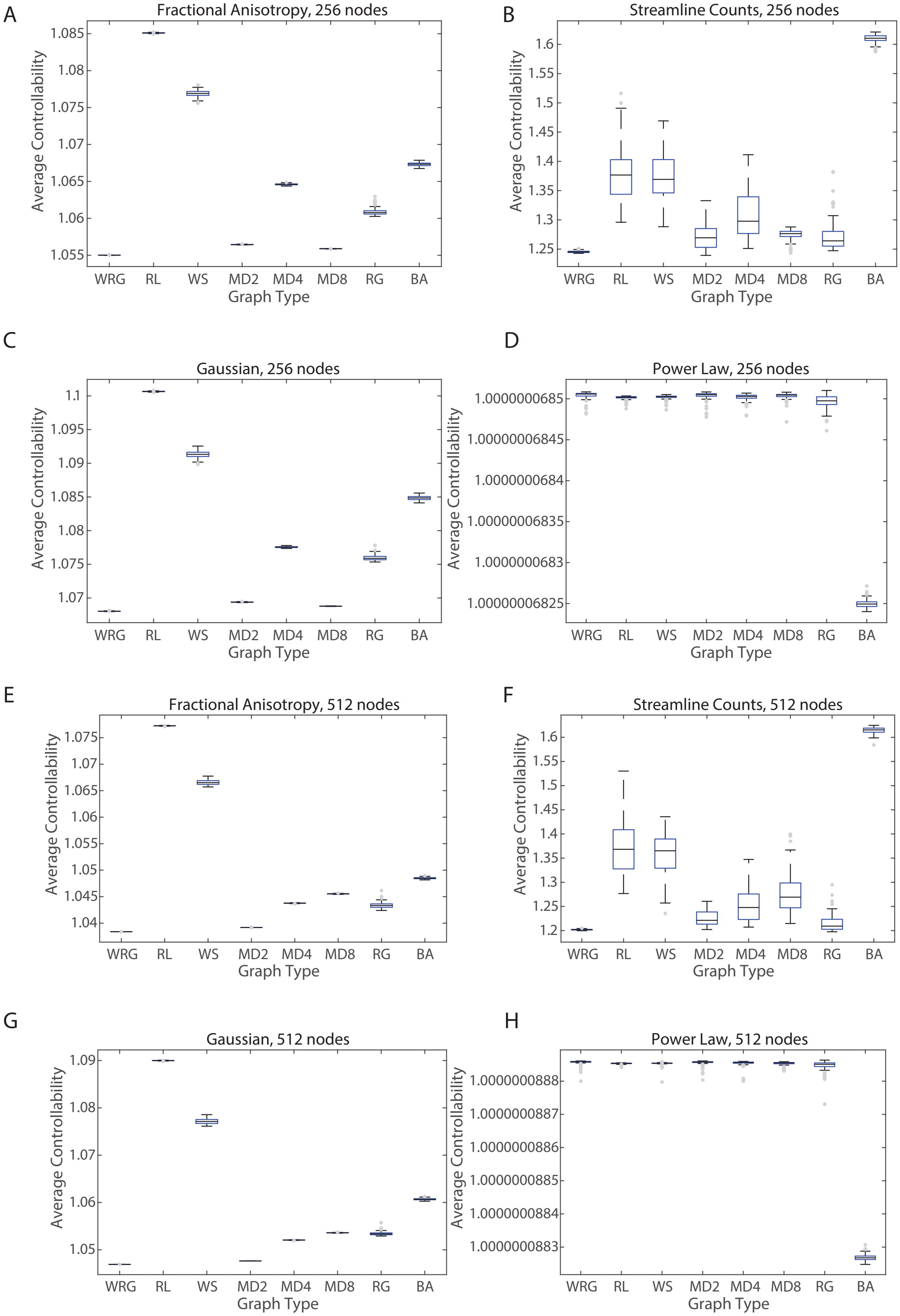

FIG. 24. **Variation in average controllability as a function of edge weighting and graph model.** Average controllability values were averaged over nodes in each graph model ensemble, and therefore boxplots show variation over graphs in the ensemble. Results are shown for four edge weighting schemes: *(A,E)* FA, *(B,F)* streamline counts, *(C,G)* Gaussian, *(D,H)* power-law. The eight graph models include the weighted random graph (WRG), the ring lattice (RL), the Watts-Strogatz small-world (WS), the modular graphs (MD2, MD4, MD8), the random geometric (RG), and the Barábasi-Albert preferential attachment (BA) models. Number of nodes is either 256 *(A-D)* or 512 *(E-H)*.

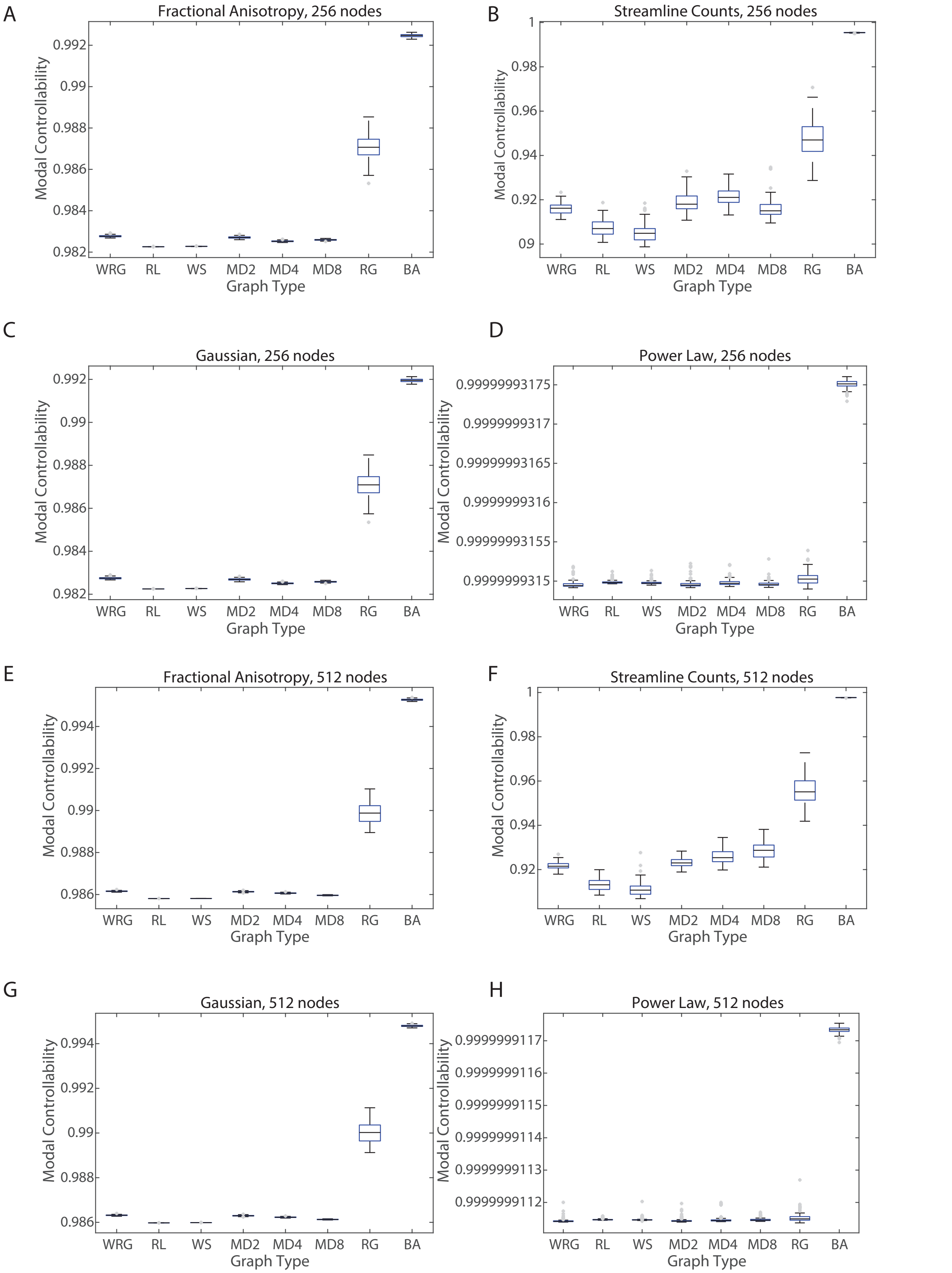

FIG. 25. **Variation in modal controllability as a function of edge weighting and graph model.** Modal controllability values were averaged over nodes in each graph model ensemble, and therefore boxplots show variation over graphs in the ensemble. Results are shown for four edge weighting schemes: *(A,E)* FA, *(B,F)* streamline counts, *(C,G)* Gaussian, *(D,H)* power-law. The eight graph models include the weighted random graph (WRG), the ring lattice (RL), the Watts-Strogatz small-world (WS), the modular graphs (MD2, MD4, MD8), the random geometric (RG), and the Barábasi-Albert preferential attachment (BA) models. Number of nodes is either 256 *(A-D)* or 512 *(E-H)*.

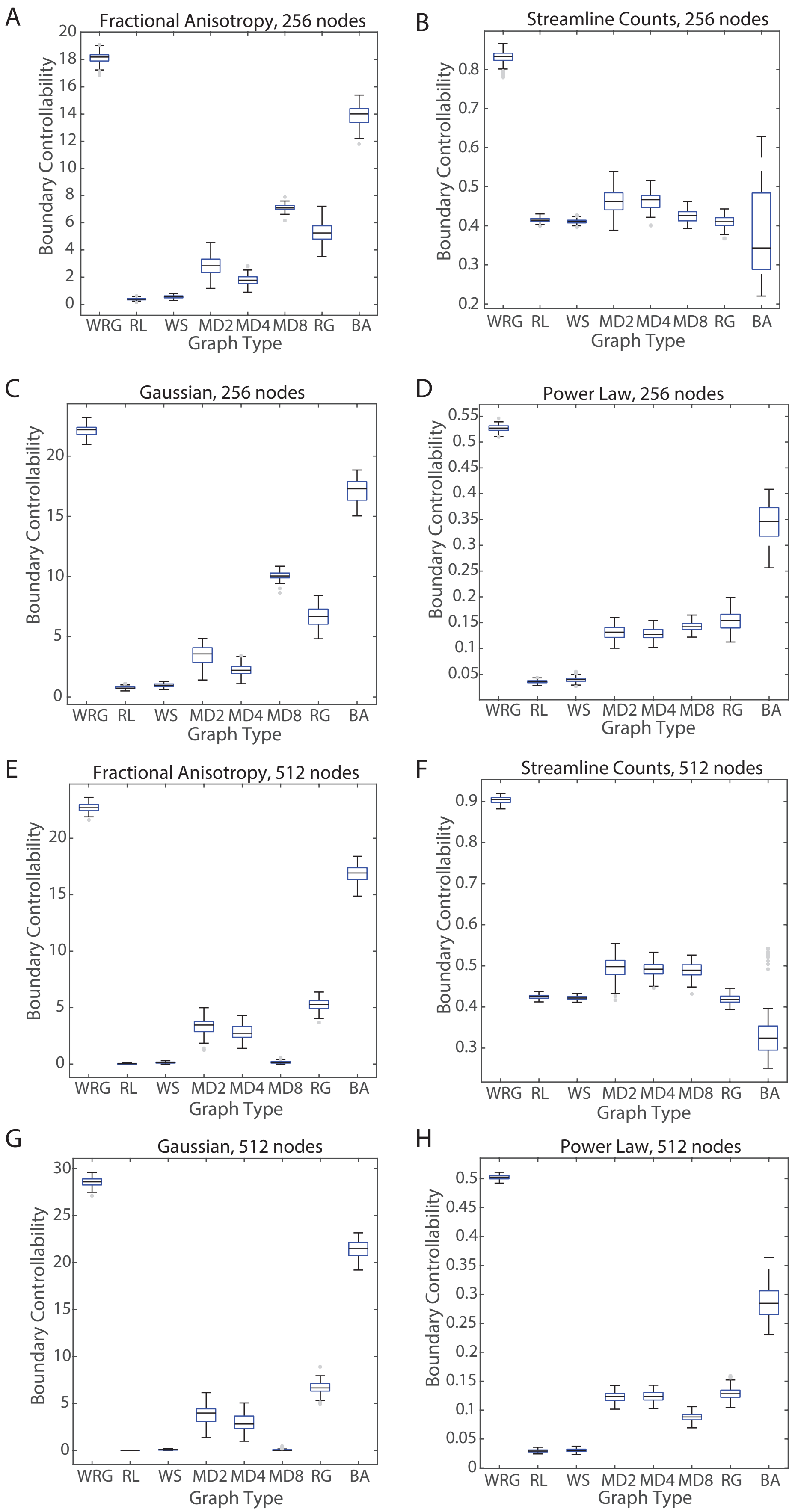

FIG. 26. **Variation in boundary controllability as a function of edge weighting and graph model.** Boundary controllability values were averaged over nodes in each graph model ensemble, and therefore boxplots show variation over graphs in the ensemble. Results are shown for four edge weighting schemes: *(A,E)* FA, *(B,F)* streamline counts, *(C,G)* Gaussian, *(D,H)* power-law. The eight graph models include the weighted random graph (WRG), the ring lattice (RL), the Watts-Strogatz small-world (WS), the modular graphs (MD2, MD4, MD8), the random geometric (RG), and the Barábasi-Albert preferential attachment (BA) models. Number of nodes is either 256 *(A-D)* or 512 *(E-H)*.

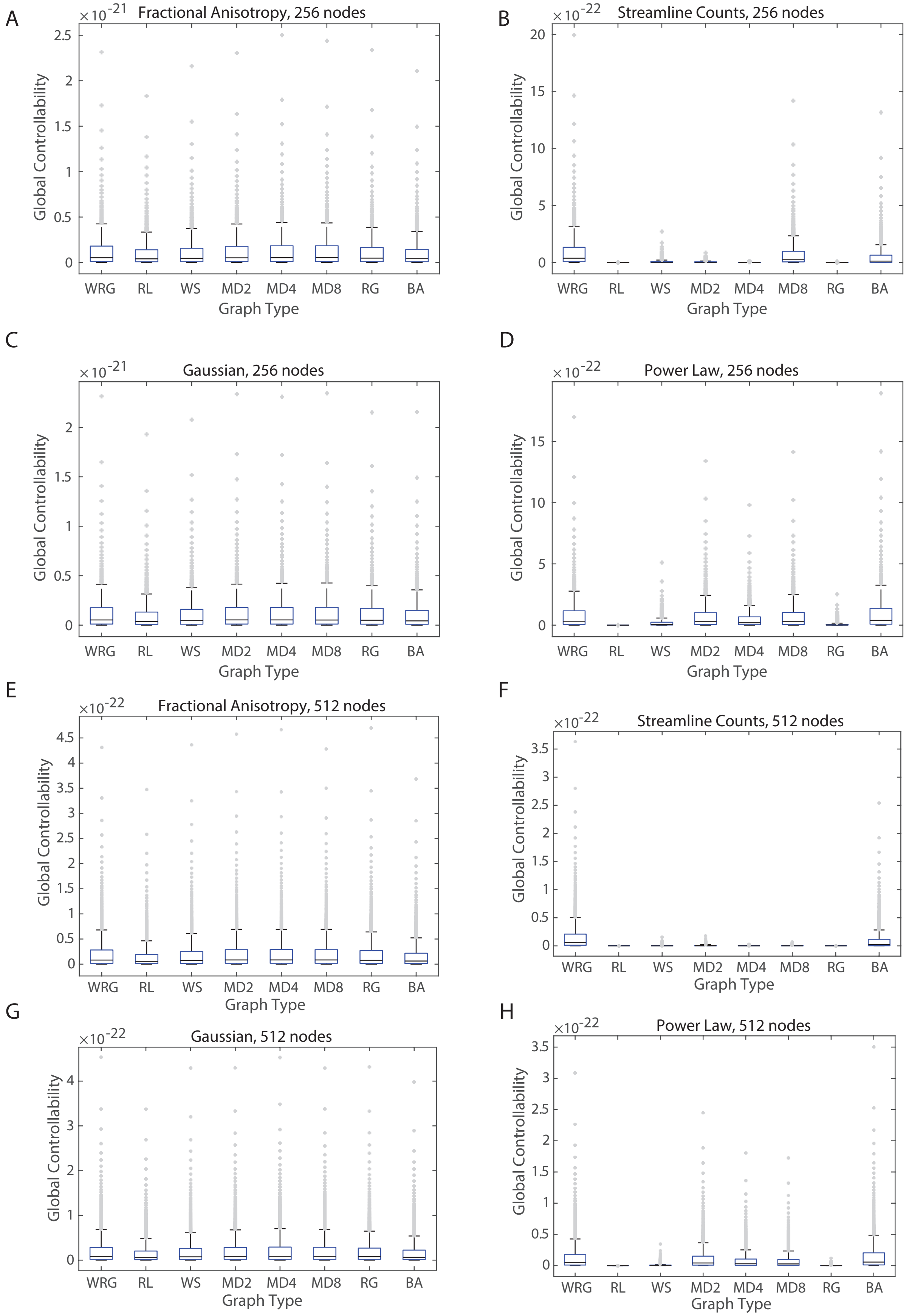

FIG. 27. **Nodal variation in global controllability as a function of edge weighting and graph model.** Global controllability values were averaged over instances in each graph model ensemble, and therefore boxplots show variation over nodes in the graph. Results are shown for four edge weighting schemes: *(A,E)* FA, *(B,F)* streamline counts, *(C,G)* Gaussian, *(D,H)* power-law. The eight graph models include the weighted random graph (WRG), the ring lattice (RL), the Watts-Strogatz small-world (WS), the modular graphs (MD2, MD4, MD8), the random geometric (RG), and the Barábasi-Albert preferential attachment (BA) models. Number of nodes is either 256 *(A-D)* or 512 *(E-H)*.

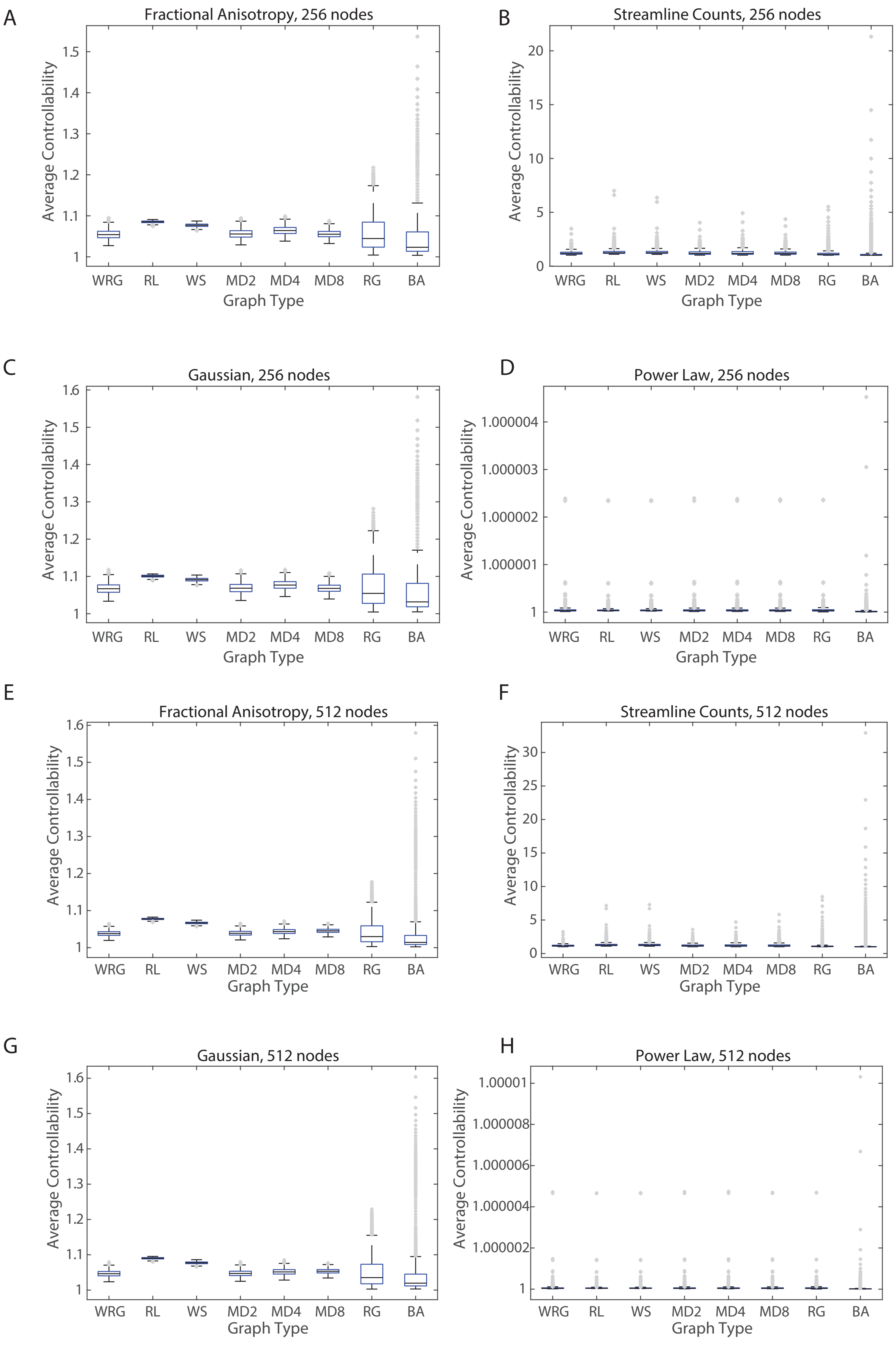

FIG. 28. **Nodal variation in average controllability as a function of edge weighting and graph model.** Average controllability values were averaged over instances in each graph model ensemble, and therefore boxplots show variation over nodes in the graph. Results are shown for four edge weighting schemes: *(A,E)* FA, *(B,F)* streamline counts, *(C,G)* Gaussian, *(D,H)* power-law. The eight graph models include the weighted random graph (WRG), the ring lattice (RL), the Watts-Strogatz small-world (WS), the modular graphs (MD2, MD4, MD8), the random geometric (RG), and the Barábasi-Albert preferential attachment (BA) models. Number of nodes is either 256 *(A-D)* or 512 *(E-H)*.

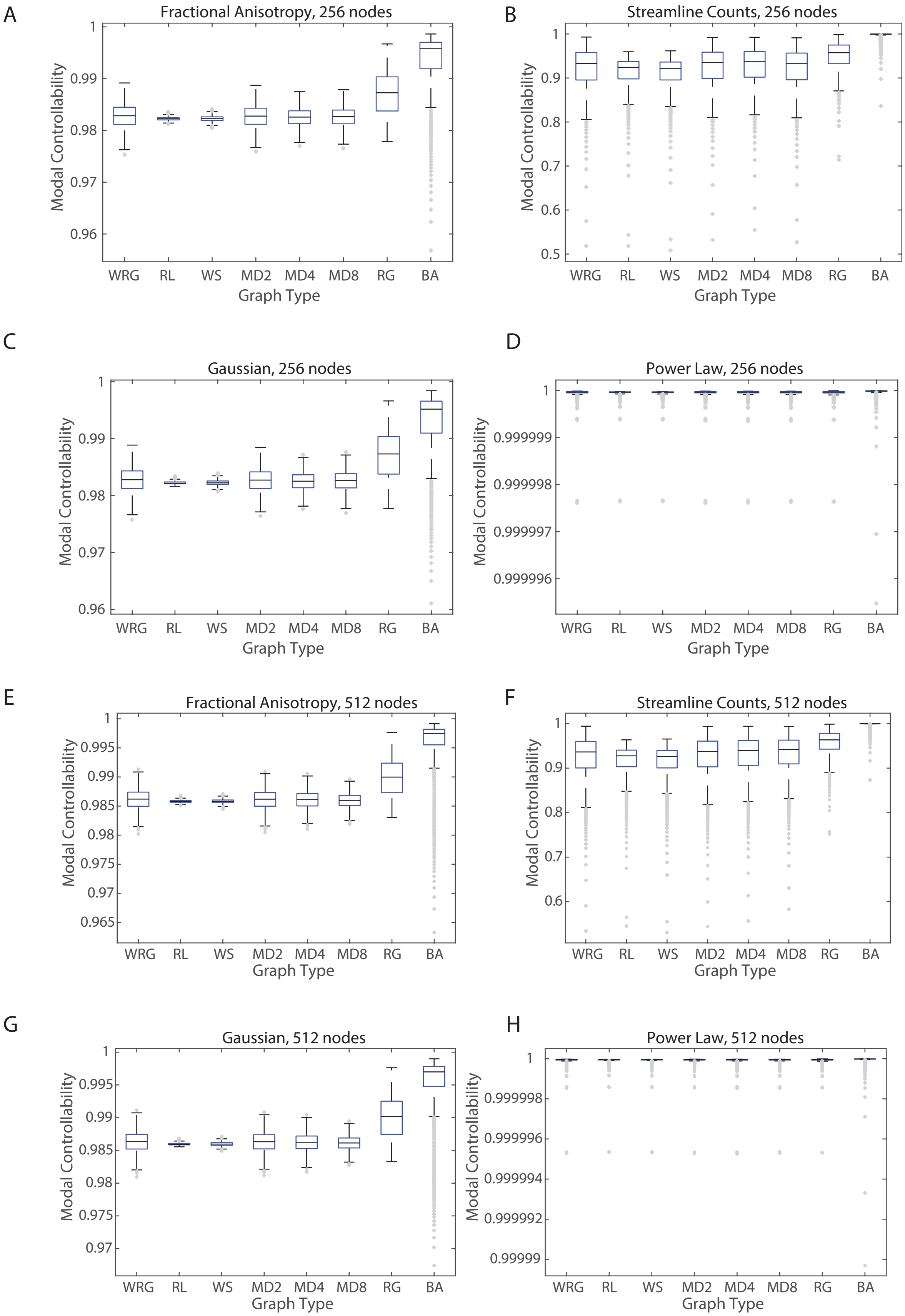

FIG. 29. **Nodal variation in modal controllability as a function of edge weighting and graph model.** Modal controllability values were averaged over instances in each graph model ensemble, and therefore boxplots show variation over nodes in the graph. Results are shown for four edge weighting schemes: *(A,E)* FA, *(B,F)* streamline counts, *(C,G)* Gaussian, *(D,H)* power-law. The eight graph models include the weighted random graph (WRG), the ring lattice (RL), the Watts-Strogatz small-world (WS), the modular graphs (MD2, MD4, MD8), the random geometric (RG), and the Barábasi-Albert preferential attachment (BA) models. Number of nodes is either 256 *(A-D)* or 512 *(E-H)*.

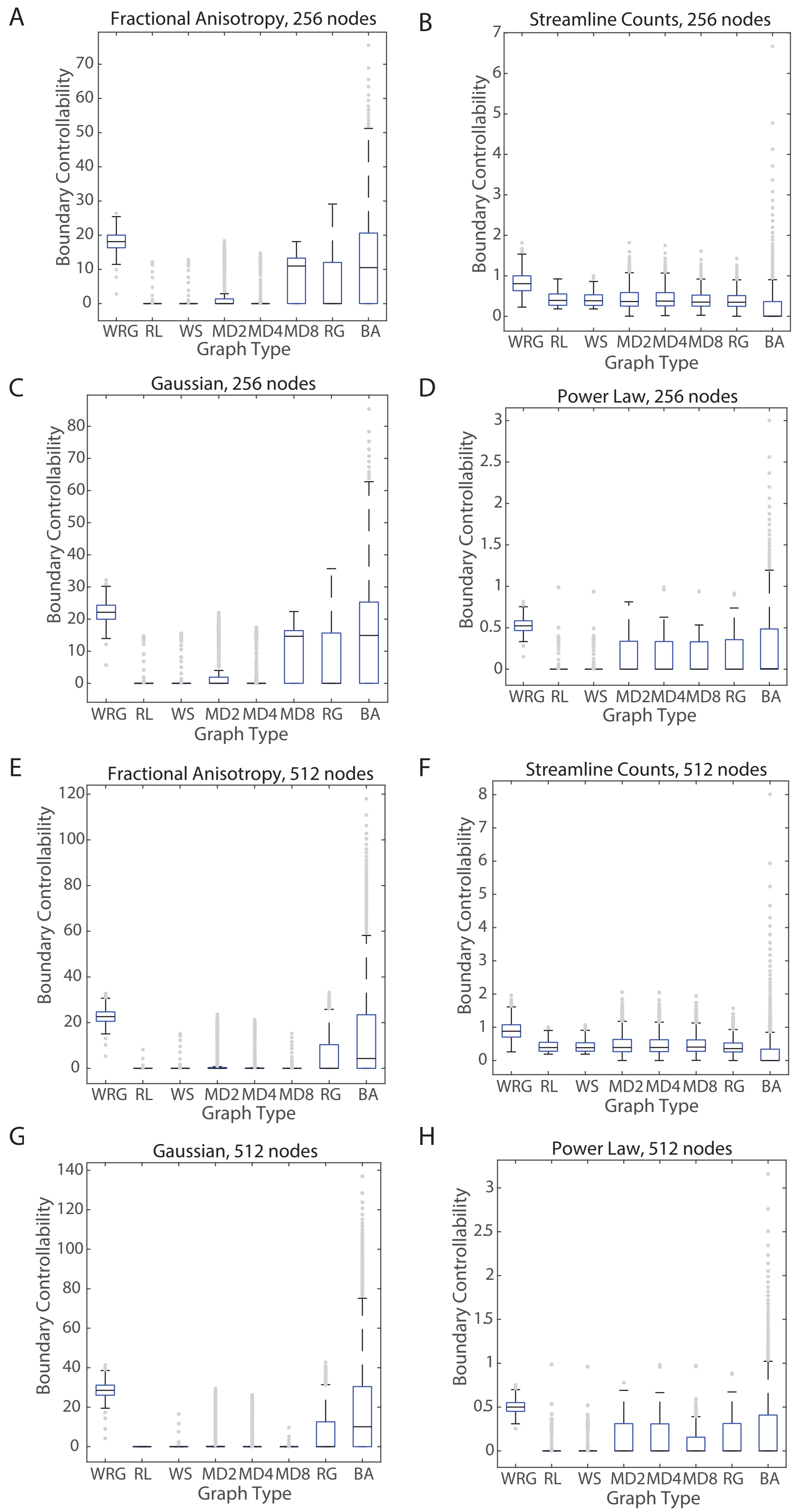

FIG. 30. **Nodal variation in boundary controllability as a function of edge weighting and graph model.** Boundary controllability values were averaged over instances in each graph model ensemble, and therefore boxplots show variation over nodes in the graph. Results are shown for four edge weighting schemes: *(A,E)* FA, *(B,F)* streamline counts, *(C,G)* Gaussian, *(D,H)* power-law. The eight graph models include the weighted random graph (WRG), the ring lattice (RL), the Watts-Strogatz small-world (WS), the modular graphs (MD2, MD4, MD8), the random geometric (RG), and the Barábasi-Albert preferential attachment (BA) models. Number of nodes is either 256 *(A-D)* or 512 *(E-H)*.

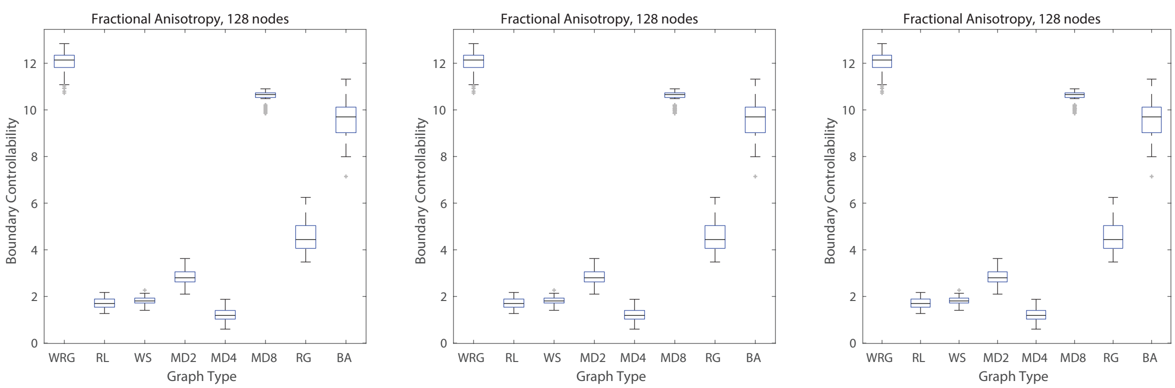

FIG. 31. **Robustness of boundary controllability estimates to variations in ρ.** *(Left)* Estimates for variation in boundary controllability over graph instances for all eight graph models weighted using the Fractional Anisotropy edge weight distribution, and calculated using $\rho = 1 \times 10^{-3}$. *(Middle)* Estimates for variation in boundary controllability over graph instances for all eight graph models weighted using the Fractional Anisotropy edge weight distribution, and calculated using $\rho = 1 \times 10^{-5}$. *(Right)* Estimates for variation in boundary controllability over graph instances for all eight graph models weighted using the Fractional Anisotropy edge weight distribution, and calculated using $\rho = 1 \times 10^{-8}$.